

Anomalous Duffing mechanics of a suspended carbon nanotube quantum dot at ultrastrong coupling

Akong N. Loh,^{*} Furkan R. Özyiğit, Fabian Stadler, Katrin Burkert, Niklas Hüttner, and Andreas K. Hüttel[†]
Institute for Experimental and Applied Physics, University of Regensburg, Universitätsstr. 31, 93053 Regensburg, Germany
 (Dated: June 30, 2026)

At cryogenic temperatures, suspended single-wall carbon nanotube quantum dots act both as prototypical quantum dots as well as high-quality factor mechanical resonators. Single-electron tunneling enables reaching an ultrastrong electron-vibron coupling regime, where the coupling parameter exceeds the vibration frequency. Due to the high quality factors, a strongly nonlinear Duffing response is easily reached. Here, we quantitatively study the Duffing response parameters of such a device and their relation to Coulomb blockade oscillation. At the edges of single-electron tunneling regions, a local increase of the Duffing parameter corresponding to a stiffening spring is observed. Size and approximate scaling of the effect agree with single-electron tunneling phenomena, which however should lead to softening spring behaviour. Possible causes of these puzzling results are discussed.

The outstanding mechanical and electronic properties of single-wall carbon nanotubes (SW-CNTs) have made them a material of choice for studying nanoelectromechanical systems at the macromolecular scale [1–6]. Their low mass, nanoscale size, extreme aspect ratio, and large mechanical quality factors at cryogenic temperatures have been exploited for ultrasensitive force, mass, and charge sensing [7–9]. Furthermore, the interaction between single-electron tunneling (SET) in a CNT quantum dot and the motion of the CNT has been studied extensively [6, 10–17]. Strong electron-vibron coupling and nonlinear mechanics of CNTs offer exciting possibilities for diverse devices, including nano-electromechanical qubits [18], quantum state transfer between degrees of freedom, high-precision sensors, sideband cooling and driving, and in general the exploration of fundamental questions in quantum mechanics [10, 16–19].

In this work, we study the mechanical response of a SW-CNT nanomechanical resonator with an embedded quantum dot. Back action of tunneling electrons causes a softening of the mechanical mode [10, 11] and demonstrates ultrastrong coupling between vibration and single-electron tunneling [20]. We obtain an electromechanical coupling parameter $g/2\pi = 2.3$ GHz and a coupling ratio $g/\omega_m = 4.0$ putting us deep in the ultrastrong coupling regime. Between the Coulomb oscillations of conductance, as a consequence of high mechanical quality factor [12] and low dynamic range [21], a nonlinear Duffing response of the electromechanical system [22] can be observed over a wide driving power range. Fitting the jump-down points of the response curve with a backbone equation, both linear and nonlinear (Duffing parameter) components of the CNT spring constant are extracted. The evolution of the nonlinear response is studied for a range of gate voltages across a Coulomb oscillation. Surprisingly, while the absolute value $|\beta(V_G)|$ of the Duffing parameter scales as expected from single-electron tunneling interactions [10], we observe a stiffening spring, that is, its sign differs from expectation.

Figure 1(a) shows a top view scanning electron micrograph of the measured device, Fig. 1(b) a larger scale sketch. A

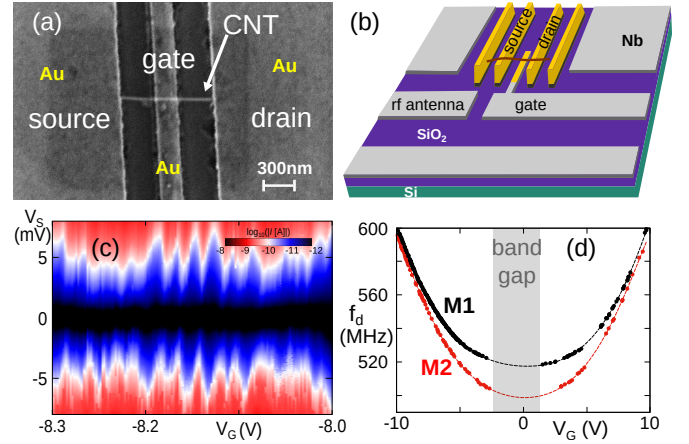


FIG. 1. (a) Top view scanning electron micrograph of a similar nanotube device, fabricated in the same batch as the measured device. The distance between source and drain electrodes is $\ell = 1 \mu\text{m}$, the nanotube to gate distance is $d = 210 \text{ nm}$. (b) Schematic drawing of the device, including a coplanar waveguide used as rf antenna and the cutting electrodes for nanotube transfer. (c) Dc current measurement showing Coulomb blockade oscillations. The absolute value of the current $I(V_G, V_{SD})$ is plotted in logarithmic scale as a function of gate voltage V_G and bias voltage V_{SD} . (d) Data points: mechanical resonance frequencies of the two observed modes M1 and M2 of the device as a function of applied gate voltage V_G , see the Supplementary Material for the measurement data. Lines: polynomial fit as guide to the eye.

CNT is grown across the prongs of a quartz tuning fork and transferred onto lithographically defined source (S) and drain (D) titanium / gold contacts with a distance of $1 \mu\text{m}$ [23]. In the region between the contacts, it is suspended over a gate electrode [16, 23]. The measurement was realized on a combined CNT – coplanar waveguide resonator device similar to these used in [16, 24, 25], however, here the additional ports only served as dc gate connection and MHz rf antenna for driving the nanotube into mechanical resonance.

At dilution refrigerator base temperature $T \approx 13 \text{ mK}$, the CNT displays typical quantum dot behaviour with moderately disordered Coulomb blockade oscillations, see Fig. 1(c). The gate lever arm is estimated as $\alpha_{\text{arm}} = 0.37$ and the charging energy as $E_C = 9 \text{ meV}$. This leads to a gate capacitance

^{*} akong.loh@ur.de

[†] andreas.huettel@ur.de

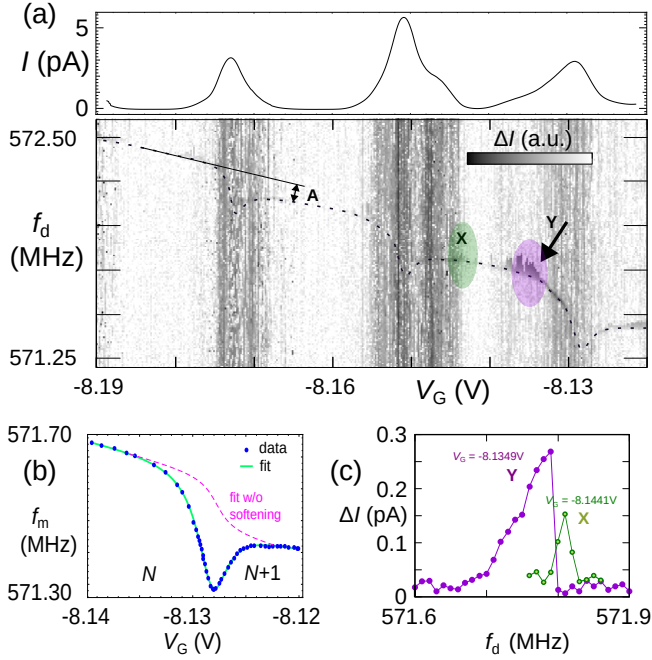


FIG. 2. Electromechanical softening of the nanotube spring constant due to single electron tunneling. (a) Upper panel: Coulomb blockade oscillations of current $I(V_G)$ for a constant bias voltage $V_{SD} = 0.5$ mV and drive frequency $f_d = 572$ MHz. Lower panel: Current $\Delta I(V_G, f_d)$ as function of gate voltage V_G and drive frequency f_d , with a constant value for each frequency sweep subtracted to enhance details. Nominal drive power $P_d = -75$ dBm and bias voltage $V_{SD} = 0.5$ mV. The dotted line is a guide to the eye for the mechanical resonance. (b) Data points: manually extracted resonance frequency points from (a) ($f_m(V_G)$) across one Coulomb peak displaying both charge-induced tension and electrostatic softening. The solid green line is a fit to the data using Eq. (1); the dashed line omits the softening term (i.e., sets $S_4 = 0$) to illustrate the tension-induced tuning alone. (c) Line cuts from (a) in the regions marked there as X and Y, illustrating a barely resolved linear response peak (X) and a nonlinear Duffing response (Y) as a function of driving frequency f_d in the current $\Delta I(V_G, f_d) = I(V_G, f_d) - \bar{I}(V_G)$.

$C_G = 6.7$ aF and a total dot capacitance $C_\Sigma = 18.1$ aF. The CNT is set in motion by a MHz drive signal coupled into the device through the nearby coplanar waveguide. The resulting nanotube oscillation amplitude strongly increases once the drive signal hits the mechanical resonance frequency. The geometric CNT–gate capacitance C_G is modulated by the position of the nanotube with respect to the gate electrode. In a dc measurement as done here, the current averaged over these oscillations is detected. Its dependence on C_G allows us to trace the CNT resonance frequency as function of V_G [2, 10, 12, 26].

Effective coupling of motion to the charge of single tunneling electrons is a direct prerequisite for many interesting experiments [16–19]. In Coulomb blockade, where $E_C \gg k_B T$ and tunneling of electrons on single-electron tunneling current peaks occurs much faster than the mechanical oscillation $\Gamma \gg 2\pi f_m$, back action of the electronic tunneling causes an electrostatic softening leading to dips in resonance frequency f_m . These dips in the mechanical resonance frequency of the

nanotube correspond to the Coulomb oscillations of conductance [10, 12].

Figure 2(a) shows a dc current measurement across three Coulomb oscillations, with a simultaneous rf driving signal of frequency f_d applied on the nearby coplanar line. The measurement was performed at a low driving power of nominally $P_d = -75$ dBm at the chip socket (corresponding to a generator power of nominally -30 dBm and approximately 45 dB input line attenuation), with the objective of observing linear oscillator response. The total dc current $I(V_G)$ at a fixed driving frequency is shown in the line plot of the upper panel; the lower panel displays the change in dc current $\Delta I(V_G, f_d)$ as function of gate voltage and driving frequency, with a constant value for each frequency sweep subtracted. A finite bias $V_{SD} = 0.5$ mV was required to obtain a mechanical resonance signal. The resonance, here in the frequency range $571 \text{ MHz} \leq f \leq 572.5 \text{ MHz}$, is traced by a dotted line as guide to the eye. Assuming a typical SW-CNT diameter of approximately 2 nm, the effective mass m of the nanotube is estimated, by multiplying the area of the CNT cylinder with the surface mass density of graphene [27, 28] which results in $m = 4.8 \cdot 10^{-21}$ kg. Using the relation $f = 1/2\sqrt{T/m\ell}$, one obtains a tension $T = 6.2$ nN on the CNT. Thus, the relatively large resonance frequency corresponds to a significant imprinted tension, most likely a result of our mechanical nanotube transfer technique [23]. This places us in the so called high tension regime [12, 16, 23, 29].

Near the Coulomb blockade oscillations, electrostatic softening of the nanotube spring constant α due to back action of tunneling electrons takes place, leading to distinct dips in resonance frequency [10, 11]. The characteristic step in the resonance frequency corresponding to the addition of one elementary charge to the quantum dot is indicated with a double arrow **A** in Fig. 2(a). The functional dependence of $f_m(V_G)$ can be modeled via the dependence of the resonance frequency on the time-averaged charge occupation $N(V_G)$ of the quantum dot with V_G , well-defined due to separation of time scales. The approach is given by [25]

$$f(V_G) = S_1 + S_2 V_G + S_3 N(V_G) + S_4 \frac{\partial N}{\partial V_G}, \quad (1)$$

where S_1 is a bare mechanical resonance frequency of the nanotube and S_2 the slope of the linear dependence of f_m on V_G . S_3 describes the size of the step in f_m across a single Coulomb oscillation, caused by an additional elementary charge on the quantum dot; cf. **A** in Fig. 2(a). Last, $S_4 = -\hbar g^2 C_\Sigma / 2\pi e C_G$ captures the frequency dip or electrostatic softening that is a result of the nanotube’s mechanical response to charge fluctuations; the magnitude of the frequency dip depends on the electromechanical coupling g , such that the fit allows us to extract the coupling parameter. Details of the derivation of S_4 are given in the supplementary material. For the bending mode considered in this work, the coupling particularly depends on how close the CNT is to the gate electrode [20, 30, 31]. Note for comparison that in [6] the working point is chosen such that there is approximately no large-scale charge dependence of the resonance frequency, in our notation corresponding to $S_2 \approx 0$ and $S_3 \approx 0$.

For modeling $N(V_G)$, we use a single Lorentz-broadened level coupled via tunnel barriers to Fermi distributions in the leads. This constructs a fit function with free parameters S_i as well as the common tunnel rate Γ that follows the evolution of quantum dot average occupation across a single Coulomb oscillation [10, 12, 16, 25]. Fig. 2(b) demonstrates this fit. Data points indicate the resonance frequencies extracted from a measurement as Fig. 2(a). The solid green line is the fit using Eq. 1. The dashed line reproduces the fit result but with S_4 set to zero to illustrate the hypothetical resonance frequency in absence of electrostatic softening. The fit works surprisingly well despite the finite applied bias $V_{SD} = 0.5$ mV [12]; this might be the case due to an asymmetry of the tunnel barriers, such that one edge of the SET region dominates the charge increase.

A nano-electromechanical system is said to be in ultra-strong electromechanical coupling when its coupling parameter $g/2\pi$ is larger than the mechanical resonance frequency f_m [17, 20, 30]. The coupling g is related to the change of the electrochemical potential μ on the quantum dot via $\mu(z) \approx \mu_0 + \hbar g z / z_{zpf}$ [20]. Here, z is the CNT deflection from equilibrium, μ_0 is the quantum dot electrochemical potential at $z = 0$, and $z_{zpf} = \sqrt{\hbar/2m\omega_m}$ is the zero point fluctuation scale of the CNT as a mechanical oscillator. From the fit of Fig. 2(b), a coupling $g/2\pi = 2.3$ GHz and a resulting coupling ratio $g/(2\pi f_m) = 4.0$ is extracted, confirming ultrastrong electromechanical coupling. This fulfils an important prerequisite for advanced nano-electromechanical experiments.

With the typical high mechanical quality factor, the drive power range for a linear, harmonic oscillator response in a carbon nanotube is very small [2, 3, 21]. Even in the carefully tuned measurement of Fig. 2(a), for some values of the gate voltage V_G a nonlinear response with the typical Duffing curve can be observed [2, 10], see Fig. 2(c), while at other values the resonant signal is below detection range. At millikelvin temperatures and increased power of the drive signal, the mechanical response of the nanotube rapidly becomes nonlinear for wide ranges of V_G [2]. This is illustrated in Fig. 3(a), plotting the dc current as function of gate voltage and drive frequency across two Coulomb blockade oscillations, now at $P_d = -55$ dBm. The nonlinear artifacts are very strong, in particular in the Coulomb blockade regions where the high amplitude branch extends far upwards in frequency, completely overshadowing the gate voltage dependence of the linear response resonance frequency. Still, the softening effects due to single-electron tunneling at the conductance maxima remain visible.

In Fig. 3(b), line cuts at fixed gate voltage $V_G = -8.1278$ V for different drive powers and sweeps of increasing drive frequency f_d , demonstrates the evolving characteristic “shark fin” Duffing response of a nonlinear resonator with stiffening spring. Here, the oscillation amplitude z derived from the resonant current is plotted; for details see [2, 16] and the Supplementary Material. For a study of the nonlinear response, the jump-down points at the high-frequency edge of the bistability region are extracted for each of the Duffing response curves and plotted in Fig. 3(c) (maximum reached motion amplitude) and Fig. 3(d) (corresponding drive frequency).

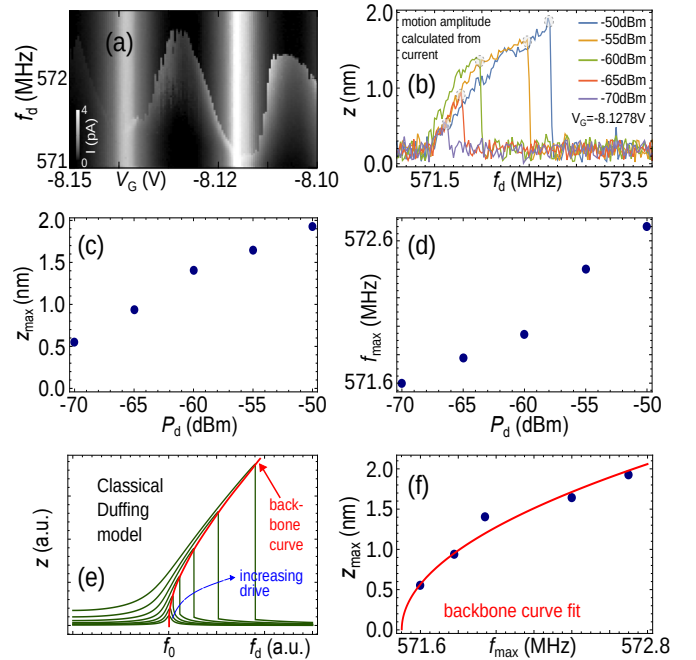


FIG. 3. (a) Nonlinear nano-electromechanical response of the nanotube device at strong driving: measured dc current $I(V_G, f_d)$ as function of gate voltage and drive frequency f_d across two Coulomb oscillations, for a rf signal of $P_d = -55$ dBm at the chip holder; dc bias $V_{SD} \approx 0$. The drive frequency f_d is always swept in increasing direction. (b) Duffing response in the oscillation amplitude for different drive powers (corresponding to line cuts in measurements such as in (a)). Again, the drive frequency f_d is always swept in increasing direction, $V_G = -8.1278$ V. (c), (d) Jump-down points of motion amplitude (c) and frequency (d) from (b), plotted against applied drive power. (e) Schematic of the drive response of a classical Duffing oscillator. (f) Example fit of a Duffing backbone curve to the jump-down points from the experiment (data from (c) and (d)).

The Duffing equation has been widely employed in the modeling and analysis of oscillating mechanical systems [29, 32–39]. Its simplest form is given by [22, 33, 40]

$$m\ddot{z} + c\dot{z} + \alpha z + \beta z^3 = F \cos(2\pi f_d t). \quad (2)$$

Here, m is the mass, z the position of the oscillating object. F is the amplitude of the driving force with frequency f_d ; c describes the (linear) damping, α the (harmonic oscillator) spring constant, and β the nonlinearity of the system. The polynomial $\alpha + \beta z^2$ represents the stiffness of the CNT spring with the linear response part controlled by α and nonlinear part controlled by the Duffing parameter β . For $\alpha > 0$ and $\beta > 0$, the spring constant of the oscillating system is said to be stiffening; conversely, for a softening system $\beta < 0$ [29, 33, 40]. Fig. 3(e) schematically displays the amplitude response curve of a stiffening Duffing system for increasing driving frequency. At strong driving, a Duffing system exhibits bistability; in the case plotted here, for increasing drive frequency, the amplitude follows the high-response branch over this region, and at its edge abruptly drops back to much lower value, resulting in the characteristic curve shape. For discussions of the case of gate voltage independent c and β in a carbon nanotube, see for

example [6, 41].

The drop-down point at the edge of the bistability region follows the so-called backbone curve as function of drive power. A theoretical expression for this curve can be derived from Eq. 2 [33, 40, 42]; one obtains

$$f_{\max}^2 = \frac{1}{4\pi^2 m} \left(\frac{3}{4} \beta z_{\max}^2 + \alpha \right). \quad (3)$$

Note that this expression does not directly contain the driving signal amplitude anymore, only the jump-down frequency and maximum amplitude. In Fig. 3(f), this backbone curve is fitted to the jump-down points in the Duffing response of the nanotube, i.e., the values from Fig. 3(c) and Fig. 3(d). Here we assume that the frequency sweep is fast enough and spontaneous switching between the two stable solutions of the Duffing equation is rare enough so the sweep always reaches the edge of the bistability region on the high-response branch. It is then possible to extract both the linear spring constant α and the Duffing parameter β ; for the chosen fixed gate voltage of $V_G = -8.1278$ V, we obtain as fit parameters $\alpha = 6.189 \cdot 10^{-2}$ kg/s² and $\beta = 8.852 \cdot 10^{13}$ kg/m²s².

Figs. 4(a-c) show the evolution of the electronic and nano-electromechanical system parameters as function of gate voltage V_G across a Coulomb oscillation. Two separate data sets are combined. The black and purple lines and points show an evaluation of the response at nonlinear driving, with $V_{SD} \approx 0$. The orange data points and lines in linear mechanical response stem from a measurement with $V_{SD} = 0.5$ mV, for better extraction of the linear resonance frequency, and have been corrected for a gate voltage offset.

Fig. 4(a) plots the measured off-resonant dc current $I(V_G)$ across a Coulomb oscillation, in combination with the extracted resonance frequency $f_m(V_G)$ in linear response at weak driving. The linear response resonance frequency can be used to calculate the corresponding spring constant via $2\pi f_m = \sqrt{\alpha_{\text{lin}}/m}$ with an estimated $m = 4.8 \cdot 10^{-21}$ kg for this device. The resulting values $\alpha_{\text{lin}}(V_G)$ are plotted together with the $\alpha(V_G)$ from Duffing backbone fits in Fig. 4(b) as consistency test. We observe reasonable agreement in magnitude and approximate functional behaviour. The Duffing evaluation leads to stronger scatter of the points as well as overall slightly higher values. The more complex evaluation procedure successfully identifies resonance peaks only at higher driving power, which for the hardening spring here indeed would lead to a higher identified value of the base resonance frequency and spring constant.

In Fig. 4(c), the Duffing parameter $\beta(V_G)$ is plotted. Additionally, the theoretically expected value $\beta_{\text{th}}(V_G)$ of the single-electron tunneling contribution is estimated from $\alpha_{\text{lin}}(V_G)$ using the relation [10]

$$\beta_{\text{th}} = \frac{1}{6} \frac{V_G^2}{C_G^2} \left(\frac{dC_G}{dz} \right)^2 \frac{d^2\alpha}{dV_G^2}. \quad (4)$$

It effectively is the third derivative with respect to z of the back action force on the quantum dot due to SET [10, 12]. While the absolute value of $\beta(V_G)$ behaves similar in both evaluations, the difference in sign is a striking deviation. Indeed, away

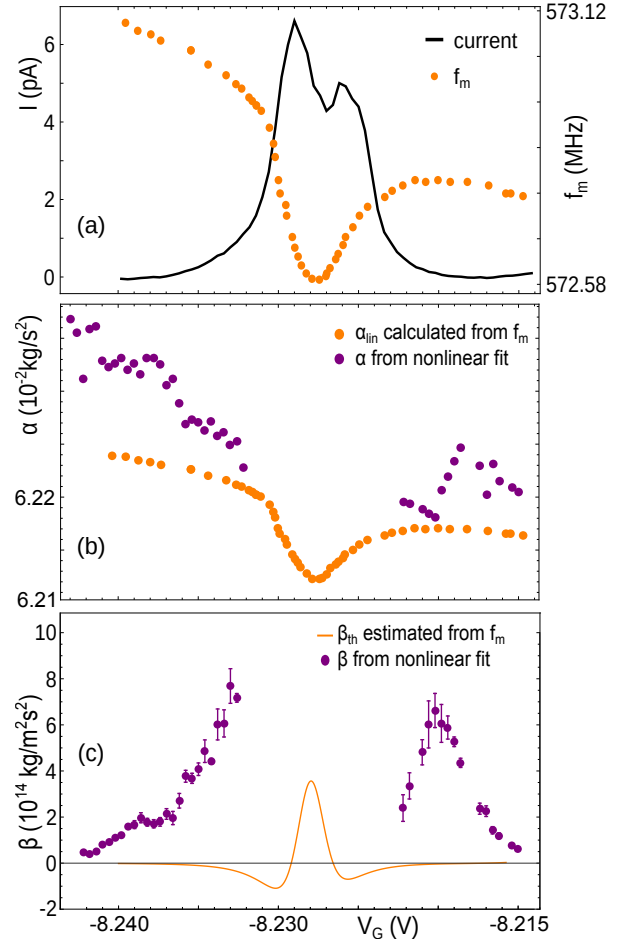


FIG. 4. Electronic and nano-electromechanical parameters at nonlinear driving as function of gate voltage V_G , for $V_{SD} \approx 0$ (black / purple). Orange data points and lines stem from a different data set in linear mechanical response with $V_{SD} = 0.5$ mV for comparison and have been corrected for a gate voltage offset. (a) dc current $I(V_G)$ and linear response resonance frequency $f_m(V_G)$. (b) Spring constant calculated from the linear response resonance frequency and extracted from Duffing response fits as in Fig. 3(f). (c) Duffing parameter $\beta(V_G)$ extracted from the Duffing response fits, and theoretical estimate of the SET Duffing parameter contribution $\beta_{\text{th}}(V_G)$ calculated from linear response, see the text.

from the center of the current peak, the SET contribution to the nonlinear behaviour should lead to a softening spring [10], while our data displays stiffening spring behaviour.

Initial publications assumed that SET always dominates the nonlinear response [10, 12, 16, 25], as compared to the non-SET related material nonlinearity which acts stiffening. In the meantime, also overall stiffening spring behaviour has been observed in experiments at low temperature [6, 41, 43, 44], with the typical explanation being that in these cases the material nonlinearity is the dominant contribution, possibly due to stronger driving. Furthermore, the material-induced nonlinear mechanical response is expected to grow with the tension in the nanotube. As a comparison, the nonlinear damping of an $l = 840$ nm CNT under tension, $T = 1.7$ nN, in *absence*

of Coulomb blockade has been studied and a nonlinear parameter $\beta = 6 \cdot 10^{12} \text{ kg/m}^2\text{s}^2$ extracted in Ref. [45], while our device is characterized by a larger value of $T = 6.2 \text{ nN}$ as mentioned above. This would however not explain the distinct gate voltage dependence of Fig. 4(c), with the material constants independent of Coulomb blockade behaviour.

An interplay of both SET and material nonlinearity effects can be considered, however it provides no clear explanation of the growth of $\beta(V_G)$ near the SET current maximum. Even assuming a straightforward addition of the contributions, the differences in feature width between observation and theory curve as well as the contributions of different sign indicate complex behaviour.

A switch in sign of the SET-induced nonlinearity is expected at the flanks of the Coulomb oscillation, indicating a transition from a softening to a hardening spring constant SET contribution or reverse, as shown in Refs. [10, 12]. In our data, no Duffing curve can be identified at the current peaks, see Fig. 4(c), leading to missing data points in the evaluation. This was also observed for several other Coulomb oscillations not shown here and may be related to nonlinear damping which should scale with nonlinearity [45]. As a result, further discussion of the gate voltage dependence of $\beta(V_G)$ enters the realm of speculation, and further experiments are required to enable a deeper understanding of this phenomenon.

In conclusion, we have studied the nonlinear mechanics of a suspended carbon nanotube quantum dot at dilution refrigerator base temperature. Motion and electron tunneling show ultrastrong coupling, at a high mechanical resonance frequency $f \sim 570 \text{ MHz}$ due to fabrication-imprinted tension. When driving, we obtain the characteristic frequency response curve of a Duffing oscillator. Fitting the Duffing backbone curve enables us to extract both linear stiffness α and Duffing parameter β as a function of gate voltage. The result demonstrates a rich interplay of Coulomb blockade, material properties and the nano-electromechanical system parameters. While displaying a clear gate voltage dependence and thus indicating SET-induced nonlinearity effects, our device shows through-

out a stiffening spring behaviour, in a puzzling deviation from expectations.

Characterization and control of the nonlinearity of a vibrating CNT with strong coupling between mechanical motion and single-electron tunneling is an important prerequisite for quantum device applications. Recently, a hybrid nano-electromechanical qubit based on a double quantum dot within a suspended CNT has been proposed [18]; the outstanding mechanical quality factors of carbon nanotubes at cryogenic temperature promise long storage times for quantum information. Correspondingly, in particular for addressing and controlling the mechanical quantum regime, the deeper understanding of the interplay of linear (i.e. resonator- or oscillator-like) and nonlinear (i.e. qubit-like) nano-electromechanical quantum phenomena in a carbon nanotube will be of central interest.

ACKNOWLEDGMENTS

The authors acknowledge financial support by the Deutsche Forschungsgemeinschaft via grants Hu 1808/4 (project id 438638106), Hu 1808/5 (project id 438640202), and SFB 1277 (project id 314695032). We would like to thank P. Hakonen for insightful discussions, and Ch. Strunk and D. Weiss for the use of experimental facilities. The measurement data was recorded using Lab::Measurement [46].

AUTHOR CONTRIBUTIONS

A. K. H. and A. N. L. conceived and designed the experiment. The coplanar waveguide device was developed and fabricated by K. B. and A. N. L., with help and advice from N. H. Nanotube growth and transfer were established and optimized by F. Ö., F. S., and A. N. L. The low temperature measurements were performed by A. N. L.; data evaluation and manuscript writing were done jointly by A. N. L. and A. K. H. The project was supervised by A. K. H.

-
- [1] V. Sazonova, Y. Yaish, H. Üstünel, D. Roundy, T. A. Arias, and P. L. McEuen, A tunable carbon nanotube electromechanical oscillator, *Nature* **431**, 284 (2004).
 - [2] A. K. Hüttel, G. A. Steele, B. Witkamp, M. Poot, L. P. Kouwenhoven, and H. S. J. van der Zant, Carbon nanotubes as ultra-high quality factor mechanical resonators, *Nano Letters* **9**, 2547 (2009).
 - [3] J. Moser, A. Eichler, J. Güttinger, M. I. Dykman, and A. Bachtold, Nanotube mechanical resonators with quality factors of up to 5 million, *Nature Nanotechnology* **9**, 1007 (2014).
 - [4] E. A. Laird, F. Kuemmeth, G. A. Steele, K. Grove-Rasmussen, J. Nygård, K. Flensberg, and L. P. Kouwenhoven, Quantum transport in carbon nanotubes, *Reviews of Modern Physics* **87**, 703 (2015).
 - [5] A. Bachtold, J. Moser, and M. I. Dykman, Mesoscopic physics of nanomechanical systems, *Reviews of Modern Physics* **94**, 045005 (2022).
 - [6] S. Sevitz, K. Aggarwal, J. Tabanera-Bravo, J. Monsel, F. Vigneau, F. Fedele, J. Dunlop, J. M. R. Parrondo, G. J. Milburn, J. Anders, N. Ares, and F. Cerisola, Sources of nonlinearity in the response of a driven nano-electromechanical resonator (2025), [arXiv:2509.12830 \[cond-mat.mes-hall\]](https://arxiv.org/abs/2509.12830).
 - [7] B. Lassagne, D. Garcia-Sanchez, A. Aguasca, and A. Bachtold, Ultrasensitive Mass Sensing with a Nanotube Electromechanical Resonator, *Nano Letters* **8**, 3735 (2008).
 - [8] P. Häkkinen, A. Isacsson, A. Savin, J. Sulkko, and P. Hakonen, Charge sensitivity enhancement via mechanical oscillation in suspended carbon nanotube devices, *Nano Letters* **15**, 1667 (2015).
 - [9] S. L. de Bonis, C. Urgell, W. Yang, C. Samanta, A. Noury, J. Vergara-Cruz, Q. Dong, Y. Jin, and A. Bachtold, Ultrasensitive Displacement Noise Measurement of Carbon Nanotube Mechanical Resonators, *Nano Letters* **18**, 5324 (2018).
 - [10] G. A. Steele, A. K. Hüttel, B. Witkamp, M. Poot, H. B. Meerwaldt, L. P. Kouwenhoven, and H. S. J. van der Zant, Strong

- coupling between single-electron tunneling and nanomechanical motion, *Science* **325**, 1103 (2009).
- [11] B. Lassagne, Y. Tarakanov, J. Kinaret, D. Garcia-Sanchez, and A. Bachtold, Coupling Mechanics to Charge Transport in Carbon Nanotube Mechanical Resonators, *Science* **325**, 1107 (2009).
- [12] H. B. Meerwaldt, G. Labadze, B. H. Schneider, A. Taspinar, Ya. M. Blanter, H. S. J. van der Zant, and G. A. Steele, Probing the charge of a quantum dot with a nanomechanical resonator, *Physical Review B* **86**, 115454 (2012).
- [13] D. R. Schmid, P. L. Stiller, Ch. Strunk, and A. K. Hüttel, Liquid-induced damping of mechanical feedback effects in single electron tunneling through a suspended carbon nanotube, *Applied Physics Letters* **107**, 123110 (2015).
- [14] G.-W. Deng, D. Zhu, X.-H. Wang, C.-L. Zou, J.-T. Wang, H.-O. Li, G. Cao, D. Liu, Y. Li, M. Xiao, G.-C. Guo, K.-L. Jiang, X.-C. Dai, and G.-P. Guo, Strongly coupled nanotube electromechanical resonators, *Nano Letters* **16**, 5456 (2016).
- [15] C. Urgell, W. Yang, S. L. De Bonis, C. Samanta, M. J. Esplandiù, Q. Dong, Y. Jin, and A. Bachtold, Cooling and self-oscillation in a nanotube electromechanical resonator, *Nature Physics* **16**, 32 (2020).
- [16] S. Blien, P. Steger, N. Hüttner, R. Graaf, and A. K. Hüttel, Quantum capacitance mediated carbon nanotube optomechanics, *Nature Communications* **11**, 1363 (2020).
- [17] C. Samanta, S. L. De Bonis, C. B. Møller, R. Tormo-Queralt, W. Yang, C. Urgell, B. Stamenic, B. Thibeault, Y. Jin, D. A. Czaplewski, F. Pistolesi, and A. Bachtold, Nonlinear nanomechanical resonators approaching the quantum ground state, *Nature Physics* **19**, 1340 (2023).
- [18] F. Pistolesi, A. N. Cleland, and A. Bachtold, Proposal for a nanomechanical qubit, *Physical Review X* **11**, 031027 (2021).
- [19] Y. Wen, N. Ares, F. J. Schupp, T. Pei, G. a. D. Briggs, and E. A. Laird, A coherent nanomechanical oscillator driven by single-electron tunnelling, *Nature Physics* **16**, 75 (2020).
- [20] F. Vigneau, J. Monsel, J. Tabanera, K. Aggarwal, L. Bresque, F. Fedele, F. Cerisola, G. A. D. Briggs, J. Anders, J. M. R. Parrondo, A. Auffèves, and N. Ares, Ultrastrong coupling between electron tunneling and mechanical motion, *Physical Review Research* **4**, 043168 (2022).
- [21] H. W. Ch. Postma, I. Kozinsky, A. Husain, and M. L. Roukes, Dynamic range of nanotube- and nanowire-based electromechanical systems, *Applied Physics Letters* **86**, 223105 (2005).
- [22] G. Duffing, *Erzwungene Schwingungen bei veränderlicher Eigenfrequenz und ihre technische Bedeutung* (Friedrich Vieweg & Sohn, Braunschweig, 1918).
- [23] S. Blien, P. Steger, A. Albang, N. Paradiso, and A. K. Hüttel, Quartz tuning-fork based carbon nanotube transfer into quantum device geometries, *Physica Status Solidi B* **255**, 1800118 (2018).
- [24] N. Kellner, N. Hüttner, M. Will, P. Hakonen, and A. K. Hüttel, Stepwise fabrication and optimization of coplanar waveguide resonator hybrid devices, *Physica Status Solidi B* **260**, 2300187 (2023).
- [25] N. Hüttner, S. Blien, P. Steger, A. Loh, R. Graaf, and A. Hüttel, Optomechanical coupling and damping of a carbon nanotube quantum dot, *Physical Review Applied* **20**, 064019 (2023).
- [26] K. J. G. Götz, D. R. Schmid, F. J. Schupp, P. L. Stiller, Ch. Strunk, and A. K. Hüttel, Nanomechanical characterization of the Kondo charge dynamics in a carbon nanotube, *Physical Review Letters* **120**, 246802 (2018).
- [27] C. Chen, S. Rosenblatt, K. I. Bolotin, W. Kalb, P. Kim, I. Kymissis, H. L. Stormer, T. F. Heinz, and J. Hone, Performance of monolayer graphene nanomechanical resonators with electrical readout, *Nature Nanotechnology* **4**, 861 (2009).
- [28] A. H. Castro Neto, F. Guinea, N. M. R. Peres, K. S. Novoselov, and A. K. Geim, The electronic properties of graphene, *Reviews of Modern Physics* **81**, 109 (2009).
- [29] R. Lifshitz and M. C. Cross, Nonlinear dynamics of nanomechanical and micromechanical resonators, in *Reviews of Nonlinear Dynamics and Complexity* (John Wiley & Sons, Ltd, 2008) Chap. 1, pp. 1–52.
- [30] G. Micchi, R. Avriller, and F. Pistolesi, Mechanical Signatures of the Current Blockade Instability in Suspended Carbon Nanotubes, *Physical Review Letters* **115**, 206802 (2015).
- [31] G. Micchi, R. Avriller, and F. Pistolesi, Electromechanical transition in quantum dots, *Physical Review B* **94**, 125417 (2016).
- [32] B. K. Jones and G. Trefan, The Duffing oscillator: A precise electronic analog chaos demonstrator for the undergraduate laboratory, *American Journal of Physics* **69**, 464 (2001).
- [33] M. Brennan, I. Kovacic, A. Carrella, and T. Waters, On the jump-up and jump-down frequencies of the Duffing oscillator, *Journal of Sound and Vibration* **318**, 1250 (2008).
- [34] J. Warminski and K. Kecik, Instabilities in the main parametric resonance area of a mechanical system with a pendulum, *Journal of Sound and Vibration Special Issue from the Second International Conference on Nonlinear Dynamics, Kharkov, Ukraine, 25-28 September 2007, Held in Honour of the 150th Anniversary of Alexander Mikhailovich Lyapunov*, **322**, 612 (2009).
- [35] M. G. Clerc, S. Coulibaly, M. A. Ferré, and R. G. Rojas, Chimera states in a Duffing oscillators chain coupled to nearest neighbors, *Chaos (Woodbury, N.Y.)* **28**, 083126 (2018).
- [36] R. Ramlan, M. J. Brennan, I. Kovacic, B. R. Mace, and S. G. Burrow, Exploiting knowledge of jump-up and jump-down frequencies to determine the parameters of a Duffing oscillator, *Communications in Nonlinear Science and Numerical Simulation* **37**, 282 (2016).
- [37] Z. Ghouli, M. Hamdi, F. Lakrad, and M. Belhaq, Quasiperiodic energy harvesting in a forced and delayed Duffing harvester device, *Journal of Sound and Vibration* **407**, 271 (2017).
- [38] L. Catalini, M. Rossi, E. C. Langman, and A. Schliesser, Modeling and Observation of Nonlinear Damping in Dissipation-Diluted Nanomechanical Resonators, *Physical Review Letters* **126**, 174101 (2021).
- [39] T. Kaisar, J. Lee, D. Li, S. W. Shaw, and P. X.-L. Feng, Nonlinear Stiffness and Nonlinear Damping in Atomically Thin MoS₂ Nanomechanical Resonators, *Nano Letters* **22**, 9831 (2022).
- [40] W. Wawrzynski, The origin point of the unstable solution area of a forced softening Duffing oscillator, *Scientific Reports* **12**, 4518 (2022).
- [41] X. Wang, L. Cong, D. Zhu, Z. Yuan, X. Lin, W. Zhao, Z. Bai, W. Liang, X. Sun, G.-W. Deng, and K. Jiang, Visualizing nonlinear resonance in nanomechanical systems via single-electron tunneling, *Nano Research* **14**, 1156 (2021).
- [42] D. W. Jordan and P. Smith, *Nonlinear Ordinary Differential Equations: An Introduction for Scientists and Engineers*, 4th ed., Oxford Scholarship Online (Oxford University Press, Oxford, 2023).
- [43] K. Willick, X. S. Tang, and J. Baugh, Probing the non-linear transient response of a carbon nanotube mechanical oscillator, *Applied Physics Letters* **111**, 223108 (2017).
- [44] G. Luo, Z.-Z. Zhang, G.-W. Deng, H.-O. Li, G. Cao, M. Xiao, G.-C. Guo, and G.-P. Guo, Coupling graphene nanomechanical motion to a single-electron transistor, *Nanoscale* **9**, 5608 (2017).
- [45] A. Eichler, J. Moser, J. Chaste, M. Zdrojek, I. Wilson-Rae, and A. Bachtold, Nonlinear damping in mechanical resonators made from carbon nanotubes and graphene, *Nature Nanotechnology* **6**, 339 (2011).

[46] S. Reinhardt, C. Butschkow, S. Geissler, A. Dirnaichner, F. Olbrich, C. Lane, D. Schröer, and A. K. Hüttel, Lab::Measurement

— a portable and extensible framework for controlling lab equipment and conducting measurements, *Computer Physics Communications* **234**, 216 (2019).